

Supplementary Materials for

Rapid fluorescence imaging of spinal cord following epidural administration of a nerve-highlighting fluorophore

Wanguo Liu¹, Rui Gu¹, Qingsan Zhu¹✉, Chunsheng Xiao²✉, Lanfeng Huang³, Xinming Zhuang⁴, Jingzhe Zhang¹, Lidi Liu⁴, Ben Ma⁵, Huailin Yang², Jianchao Ma¹, Zhipeng Hu², Chenglin Tang¹✉, Shuhua Zhao⁶✉, Xuesi Chen²

1. Department of Orthopaedic Surgery, China-Japan Union Hospital, Jilin University, Changchun, China.
2. Key Laboratory of Polymer Ecomaterials, Changchun Institute of Applied Chemistry, Chinese Academy of Sciences, Changchun, China.
3. Department of Orthopaedic Surgery, The Second Hospital, Jilin University, Changchun, China.
4. Department of Orthopaedic Surgery, The First Hospital, Jilin University, Changchun, China.
5. Department of Orthopaedic Surgery, Jinhua Central Hospital, Zhejiang University, Jinhua, China.
6. Department of Occupational and Environmental Health, Public Health School, Jilin University, Changchun, China.

✉Corresponding author

Email Addresses: zhuqs@jlu.edu.cn (Q. Zhu), xiaocs@ciac.ac.cn (C. Xiao), tcl6056@jlu.edu.cn (C. Tang), shzhao@jlu.edu.cn (S. Zhao)

Supplementary Figures

Figure S1. Kinetic study of BMB imaging of spinal cord after epidural administration of BMB at 50 µg/rabbit (in BMB-m formulation).

Figure S2. The images of spinal cord and surrounding tissues after epidural administration of BMB (50 µg/rabbit, in BMB-m formulation, n=3).

Figure S3. The images of spinal cord and surrounding tissues after intravenous administration of BMB (5.0 mg/rabbit, n=3).

Figure S4. Detection of BMB in representative organs.

Figure S5. The white light and fluorescence imaging were observed at the lumbar nerve roots.

Figure S6. Confocal laser scanning microscope (CLSM) observations of transverse sections of spinal cord at different segments.

Figure S7. Detection of BMB in CSF obtained from the cerebellomedullary cistern.

Figure S8. Cell viability assays.

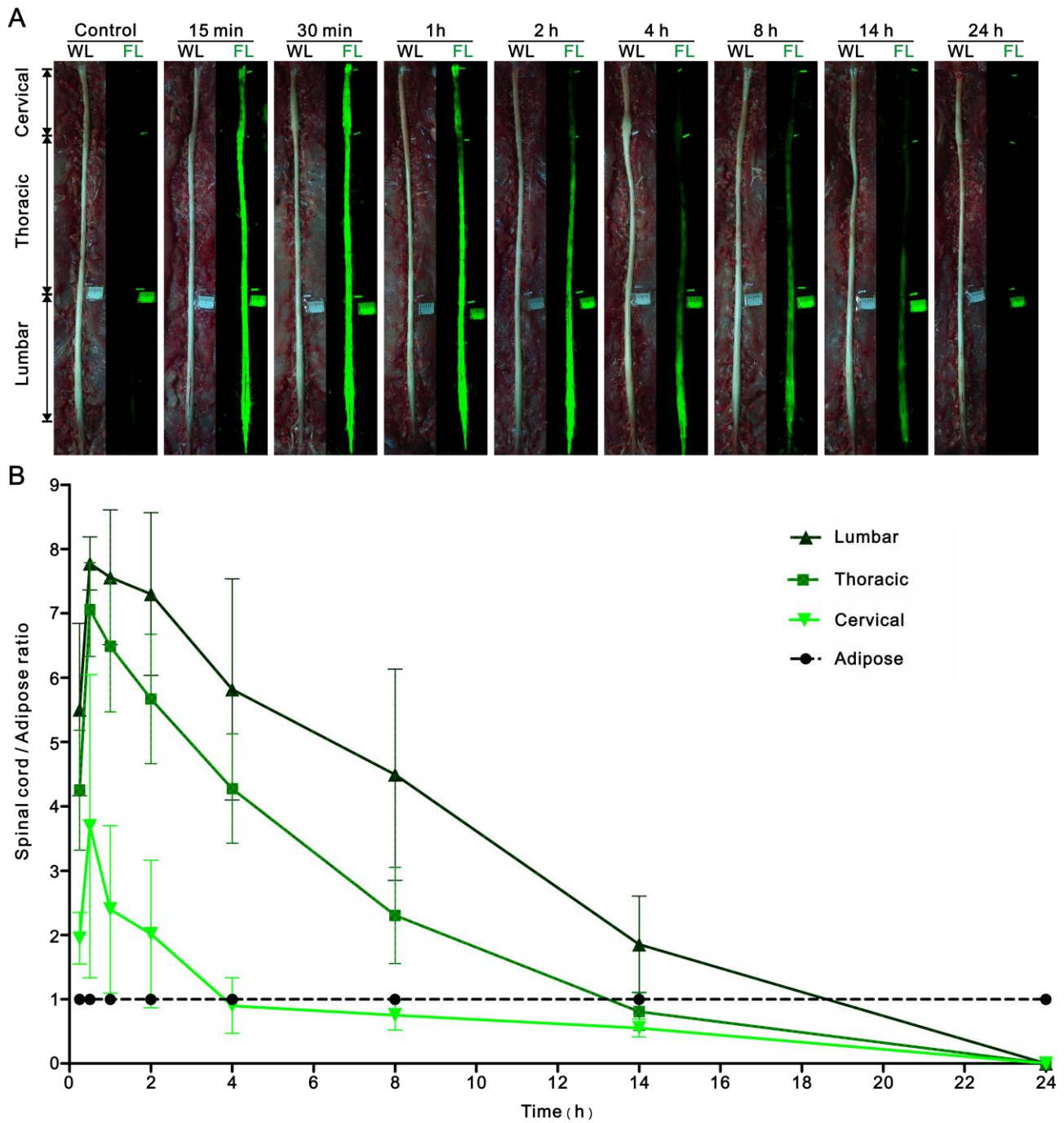


Figure S1. Kinetic study of BMB imaging of spinal cord after epidural administration of BMB at 50 $\mu\text{g}/\text{rabbit}$ (in BMB-m formulation). **(A)** Observation of the spinal cord under white or UV light at different time intervals. The complete imaging of spinal cord is observed at the time as short as 15 min. **(B)** The fluorescence ratio of spinal cord to adipose (SC/A) at the lumbar, thoracic and cervical segments at different times. The highest SC/As are observed at 30min post-injection of BMB-m solution. Meanwhile, the meaningful imaging (SC/A ratio > 2) of lumbar, thoracic and cervical could last up to 14, 8 and 2 hours, respectively. Data shown represent mean \pm SD of at least three experiments. WL: white light; FL: fluorescence.

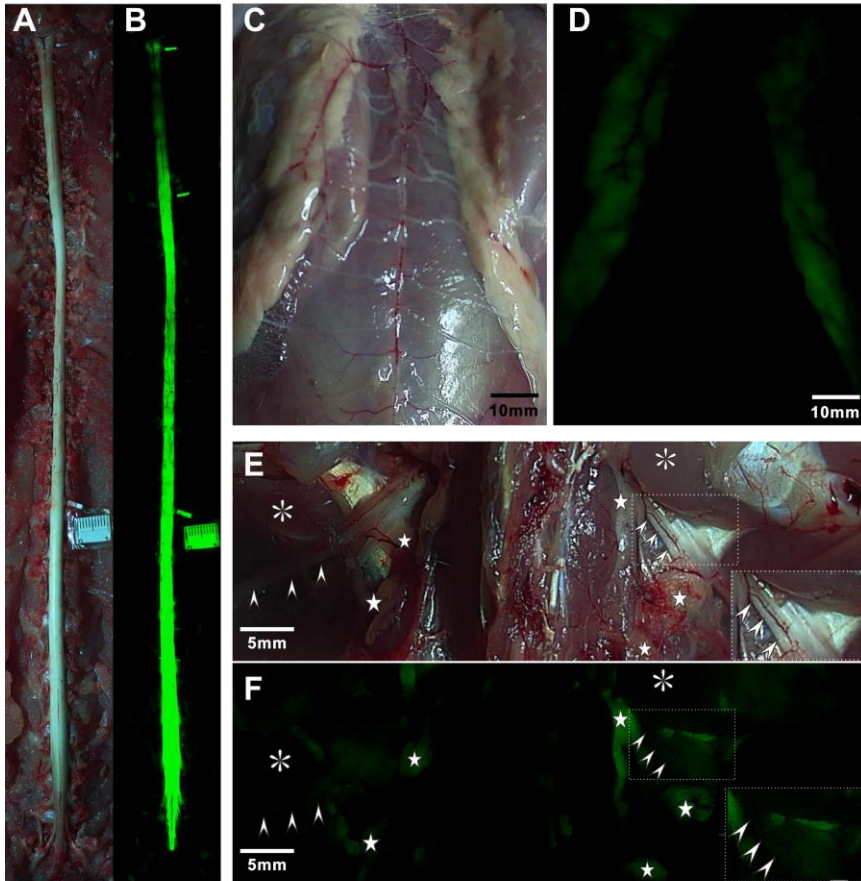


Figure S2. The images of spinal cord and surrounding tissues after epidural administration of BMB (50 $\mu\text{g}/\text{rabbit}$, in BMB-m formulation, $n=3$). The white light and fluorescence images were taken at 30 min post-injection for spinal cord (**A**, **B**), dorsal adipose tissue (**C**, **D**) and sciatic nerve (**E**, **F**). Fluorescence imaging of spinal cord was clearly observed with a SC/A ratio at 6.7 (**B**). Visible auto-fluorescence was observed in the adipose tissues at both the dorsal part (**D**) and surrounding of sciatic nerve (**F**, indicated by stars). Almost no fluorescence was observed in muscle (**B**, **D** and **F**, indicated by asterisks) and sciatic nerve (**F**, indicated by arrowheads).

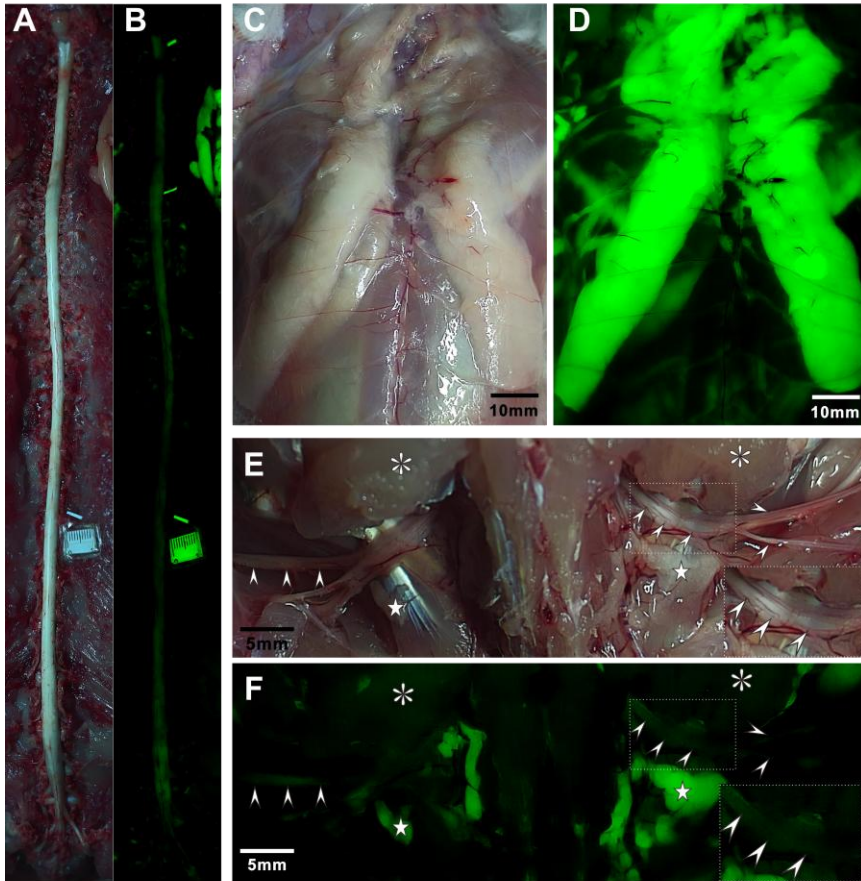


Figure S3. The images of spinal cord and surrounding tissues after intravenous administration of BMB (5.0 mg/rabbit, n=3).The white light and fluorescence images were taken at 4 h post injection for spinal cord (**A, B**), dorsal adipose tissue (**C, D**) and sciatic nerve (**E, F**). A weak fluorescence was observed in the spinal cord with a SC/A ratio at 0.35, which was much lower than that obtained by epidural administration (SC/A ratio = 6.7, see supplementary Figure 8). The significantly enhanced fluorescence was observed in the adipose tissues at both the dorsal part (**D**) and surrounding of sciatic nerve (**F**, indicated by stars). A weak fluorescence was also visible in the muscle (**D** and **F**, indicated by asterisks) and sciatic nerve (**F**, indicated by arrowheads). All these observations indicated that the BMB lacks targeting to the spinal cord when administrated intravenously.

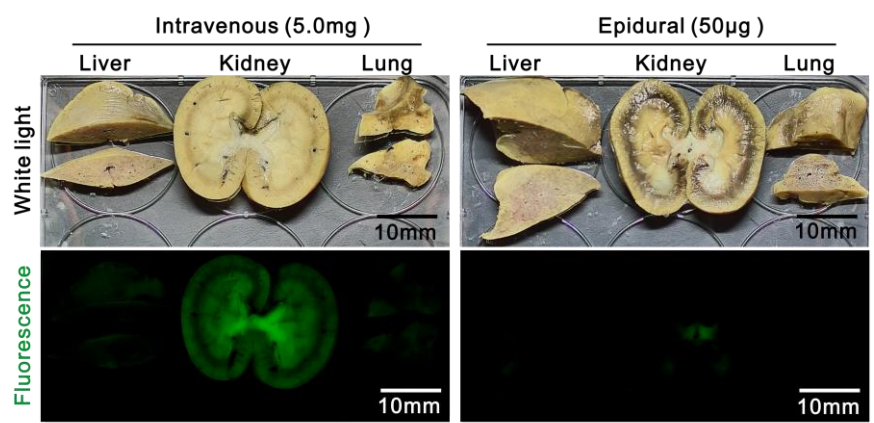


Figure S4. Detection of BMB in representative organs. White light and fluorescence images of liver, kidney and lung after treatment with BMB (in BMB-m formulation) using different administration methods. Compared with epidural administration, obvious fluorescence was observed for organs from the group treated with intravenous injection of BMB-m.

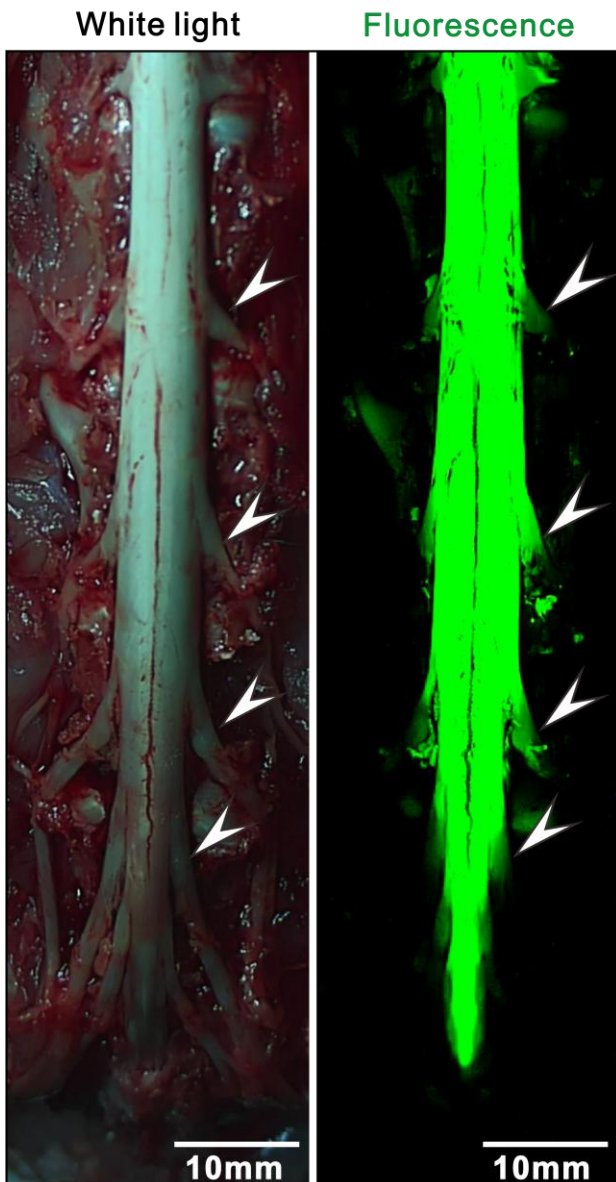


Figure S5. The white light and fluorescence imaging were observed at the lumbar nerve roots. The fluorescence signal was found to be ended at the dorsal root ganglions (arrowheads).

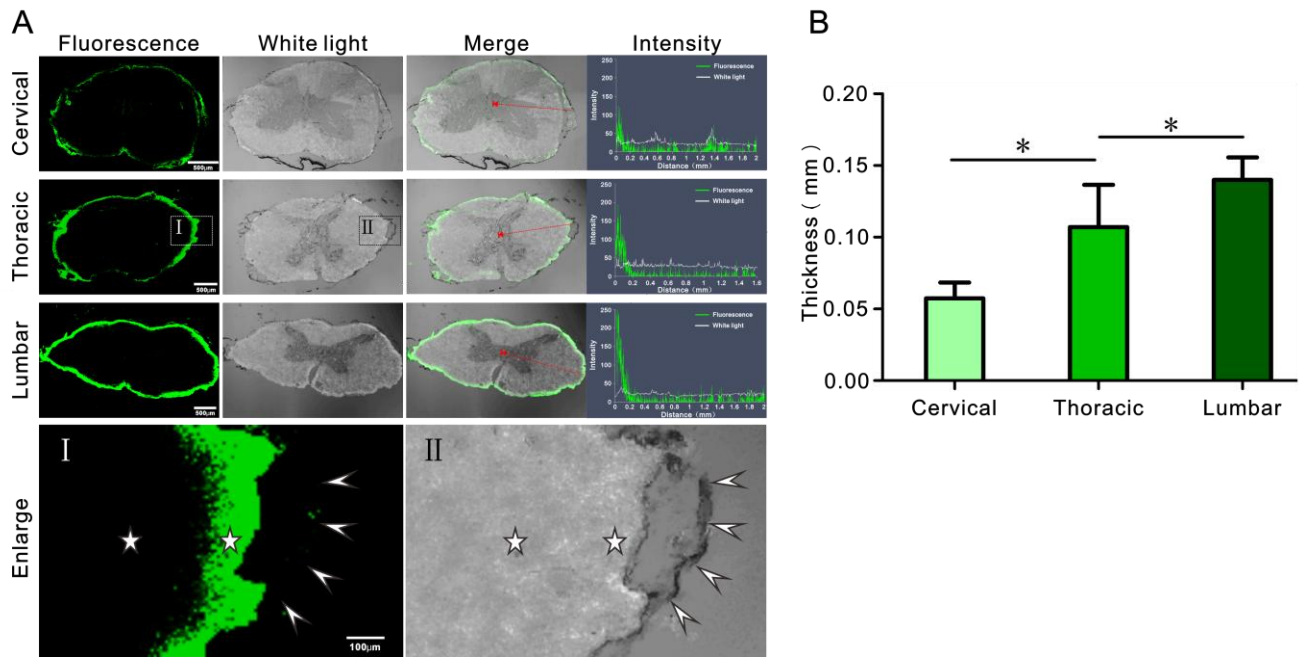


Figure S6. Confocal laser scanning microscope (CLSM) observations of transverse sections of spinal cord at different segments. **(A)** The CLSM images and the fluorescence intensity of the sections at lumbar, thoracic and cervical site, respectively. The fluorescence intensities exhibit a decreasing gradient from lumbar to cervical segment. The enlarged images are showed in I and II. It is clearly observed that the BMB is bound mainly in the peripheral region of white matter (indicated by stars), while weak fluorescence was detected in the meninges (indicated by arrowheads). **(B)** The staining thickness on the rim of spinal cord at different sections. There is significant difference between each section. * $P < 0.05$ (one-way ANOVA with Newman-Keuls).

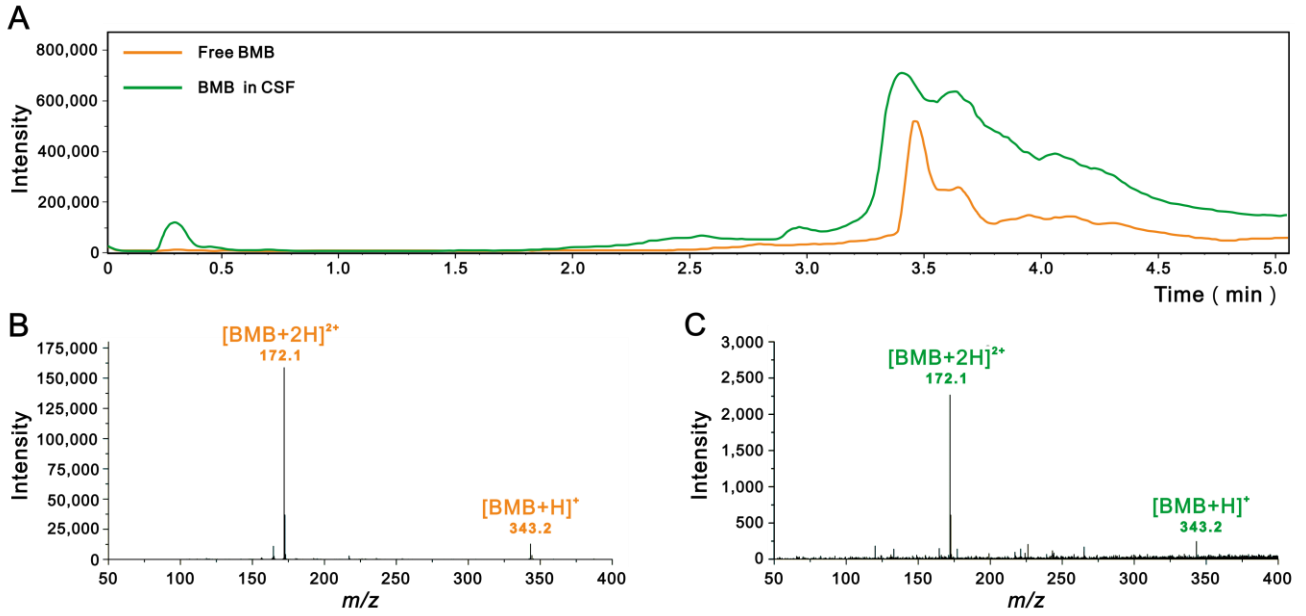


Figure S7. Detection of BMB in CSF obtained from the cerebellomedullary cistern. **(A)** The total ion current (TIC) chromatogram of free BMB and CSF sample obtained from the cerebellomedullary cistern. **(B)** The electrospray ionization mass spectrum of free BMB sample at 3.5 min of TIC chromatogram. **(C)** The electrospray ionization mass spectrum of CSF sample at 3.5 min of TIC chromatogram. Both **(B)** and **(C)** showing typical ion signals corresponding to $[BMB+2H]^{2+}$ and $[BMB+H]^+$, indicating the presence of BMB in CSF in the cerebellomedullary cistern.

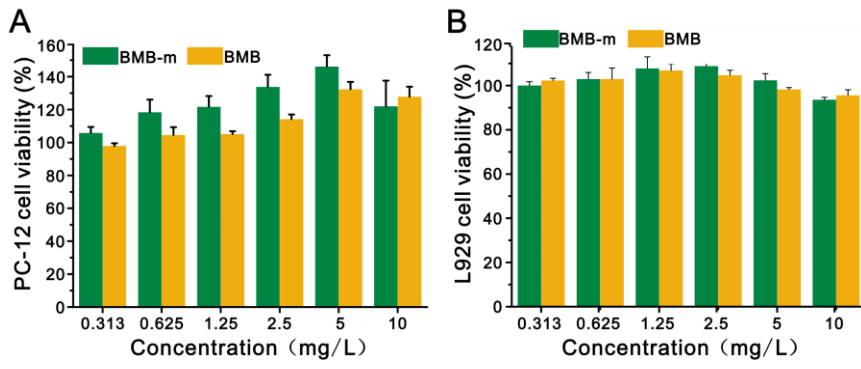


Figure S8. Cell viability assays. The BMB showed low cell cytotoxicities toward both PC-12 **(A)** and L929 cells **(B)**.